CHAPTER 4

STUDY OF THE EFFECT OF IONIC STRENGTH ON AB_{1-42} PEPTIDE AGGREGATION

Study of the effect of ionic strength on $A\beta_{1-42}$ peptide aggregation

4.1. Abstract:

Numerous neurodegenerative diseases may develop as a result of the accumulation of misfolded proteins in cells under stressful conditions. Amyloid-Beta ($A\beta_{1-42}$) peptide, the disease-causing agent of AD, has a tendency to fold into β-sheets under stress, resulting in aggregated amyloid plaques. This is affected by variables like pH, temperature, metal ions, residue mutation, and the solution's ionic strength. Numerous studies have emphasized the significance of ionic strength in influencing the tendency of $A\beta_{1-42}$ peptide for folding and aggregation. Hence, there was a need to understand the effect of ionic strength of the solution on the aggregation propensity of $A\beta_{1-42}$ peptide at the molecular level. Therefore, this computational study have been performed for a clear understanding of the effect of ionic strength of the solution on the aggregation propensity of $A\beta_{1-42}$ peptide using Molecular Dynamics (MD) Simulation. In this study, MD simulations were performed on $A\beta_{1-42}$ peptide monomer placed in (i) 0 M, (ii) 0.15 M and (iii) 0.30 M concentration of NaCl solution. To prepare the input files for the MD simulations, the Amberff99SB force field have been used. The conformational dynamics of $A\beta_{1-42}$ peptide monomer in different ionic strength of the solutions were illustrated from the analysis of the corresponding MD trajectory using CPPTRAJ tool. From the MD trajectory analysis, it is observed that with an increase in the ionic strength of the solution, $A\beta_{1-42}$ peptide monomer shows a lesser tendency to undergo aggregation. From the RMSD and the SASA analysis, it has been noticed that $A\beta_{1-42}$ peptide monomer underwent a rapid change in conformation with increase in the ionic strength of the solution. In addition, from the radius of gyration (R_g) analysis, it has been observed that the $A\beta_{1-42}$ peptide monomer is more compact at moderate ionic strength of the solution. The $A\beta_{1-42}$ peptide is also found to hold its helical secondary structure at moderate and higher ionic strength of the solution. The diffusion coefficient of $A\beta_{1-42}$ peptide monomer was also found to vary with the ionic strength of the solution. A relatively higher diffusion coefficient value was observed for $A\beta_{1-42}$ peptide at moderate ionic strength of the solution. The findings from this computational study highlight the marked effect of ionic strength of the solution on the conformational dynamics and aggregation propensity of $A\beta_{1-42}$ peptide monomer.

4.2. Introduction:

The improper folding of proteins is a significant phenomenon that has been linked to the development of a wide variety of diseases. These diseases include cancers, cardiovascular diseases, metabolic disorders, and various neurodegenerative disorders. Misfolded proteins can become clumped together into aggregates when the normal conditions of the cell are disrupted and the protein quality control system of the cell is unable to keep the protein homeostasis in the cell stable [533-535]. Because of their potential usefulness in medical treatment, the cellular pathways that are used to transport and remove misfolded proteins are the subject of extensive research. Amyloid plaques are one of the proteinaceous aggregates that can build in the brain cells and eventually lead to dementia as a result of this accumulation. AD and other forms of dementia are serious issues in neurodegenerative illnesses. AD, the most common form of dementia, is thought to be responsible for between 60 to 70 percent of cases, as reported by the World Health Organization (WHO). The WHO has stated in factsheets that dementia affects roughly 60-70% of the elderly population and that approximately 10 million new cases of dementia are diagnosed each year. Memory loss, changes in mood and behavior, difficulties with communication, increased anxiety and/or anger, and an increased need for more time to do daily chores are just some of the problems that an AD patient will begin to experience as the condition develops. Loss of bodily functions ultimately leads to the patient's death as the patient's condition continues to deteriorate. The age at which a person is diagnosed with AD is the single most important factor in determining that individual's lifetime [536].

Amyloid plaques are a pathological hallmark of AD, as they are of a number of other neurodegenerative illnesses [533]. It has been discovered that the peptide known as Amyloid-Beta (Aβ) makes up the majority of amyloid plaques. Amyloids exist as intracellular inclusions or extracellular plaques (amyloid). These amyloid deposits are the root cause of an aberrant accumulation of proteins in tissues, which ultimately results in organ malfunction and death. The huge membrane-spanning glycoprotein known as Amyloid Precursor Protein (APP) is cleaved into smaller and smaller pieces, and gradually Aβ peptide is formed. This Aβ peptide can be found in two different isoforms, which are designated as $A\beta_{1-40}$ (which contains 40 amino acid residues) and $A\beta_{1-42}$ (which contains 42 amino acid residues). These two isoforms each have their own unique

process for oligomerization [537, 538]. Between the two isoforms, the aggregation of the $A\beta_{1-42}$ peptide has been discovered to be the more significant and hazardous of the two, as well as the primary component of senile plaques [539-541]. The production of regular fibrils is typically the consequence of Aβ monomers aggregating into a variety of oligomer forms, which in turn leads to the formation of Aβ fibrils. However, it has been discovered that the Aβ peptides share a common structural motif as well as the aggregation process. This helps in understanding the pathogenic mechanism as well as the disease-specific components. Many of the later studies on the structural organization of disease-related amyloid fibrils have highlighted the identification of the exact register motif. This is because the pathways by which Aβ peptides aggregate are generally influenced by the primary amino acid sequence and the intermolecular interactions. NMR and molecular dynamics experiments have provided the majority of the structural information that we have regarding Aβ peptides. Aβ42's C-terminus is more structured than Aβ40's C-terminus because residues 31-34 and 38-41 form a β-hairpin, reducing the flexibility of the C-terminal region. This may be the cause of the greater aggregation propensity of Aβ42 than Aβ40. NMR-guided simulations have suggested the conformational states of Aβ peptides ($A\beta_{1-40}$ and $A\beta_{1-42}$). The $A\beta_{1-42}$ peptide has the propensity to fold incorrectly into β-sheets, which can then aggregate to produce hazardous oligomers and, ultimately, mature amyloid fibrils [542-544]. Several experiments, such as nuclear magnetic resonance spectroscopy (NMR), X-ray crystallography, circular dichroism (CD), electron microscopy (EM), transmission electron microscopy (TEM), ion mobility mass spectrometry (IM-MS), and atomic force microscopy (AFM) measurements, have been done to study and analyze the initial seed structure of the $A\beta_{1-42}$ peptide that can cause aggregation [545]. Because there are so many different types of aggregates and the process is sensitive to a wide range of environmental conditions, studying the conformational changes that happen when $A\beta_{1-42}$ peptides clump together is a very difficult task that requires a high level of expertise to complete. The widespread availability of various homologous peptide conformations, the stringent regulation of experimental parameters, and the relatively shorter duration required for the analysis of desired protein sequences are all factors that significantly facilitate the use of computational tools in today's scientific research [536]. Several factors influence a polypeptide's ability to form amyloid, including a high β-sheet propensity, a lack of prolines, a low net charge, and a strong amyloidogenic propensity [547, 548]. The rate of the amyloid formation may be triggered by the changes in the

local environment of a normally soluble polypeptide [549]. These changes can be determined by several factors, such as pH, pressure, temperature, changes in the solvent or co-solvent composition, interaction with membranes or components of the extracellular matrix, and also changes in ionic strength [550, 551]. Amyloid fibril structured regions frequently adopt parallel arrangements rich in β-strands, resulting in quasi-infinite arrays of identical residues between adjacent polypeptide chains [552]. These arrangements suggest the presence of significant ionic interactions in amyloids. Ionic strength-dependent studies of amyloid formation have suggested that ions can influence the kinetics and thermodynamics of the aggregation process [543-545]. The effect of ionic strength, however, varies from protein to protein. There are studies that highlight the importance of ionic strength on the folding propensity and aggregation of $A\beta_{1-42}$ peptide. Therefore, the influence of ionic strength of the solution on the aggregation propensity of $A\beta_{1-42}$ peptide (PDB ID-1IYT) have been studied using three different concentrations of NaCl (0 M, 0.15 M, and 0.30 M) [546]. The 0.15 M NaCl concentration of solution has been used to mimic the physiological conditions and the high concentration of NaCl (0.30 M) as a model of intracellular conditions under stimulated conditions. Such a high ionic strength of solution was used in this study to investigate the limit in which the long range electrostatic interactions affect the structure of the $A\beta_{1-42}$ peptide monomer. The three systems were then subjected to 40 ns molecular dynamics simulation to analyze the conformational dynamics of $A\beta_{1-42}$ peptide in three different ionic strengths of the solution.

4.3. Materials and Methods

4.3.1. Preparation of the Initial Structures:

In the RCSB protein data bank [502, 503], a number of $A\beta_{1-42}$ structures are available. And so far, an X-ray crystal structure for the full $A\beta_{1-42}$ sequence does not exist, but monomers as well as fibril nuclear magnetic resonance (NMR) structures are available for the full-length $A\beta_{1-42}$. A 3-D structure of $A\beta_{1-42}$ peptide (PDB 1IYT) (chain A, total models: 10) [547] was selected to be used as an initial structure for molecular dynamics simulation, as this has been the NMR structure in an apolar microenvironment and has been used widely in a larger number of computational studies in the literature. This $A\beta_{1-42}$ peptide model NMR structure was viewed in UCSF Chimera package alpha

v.1.12 [530], and amongst an ensemble of 10 models present in chain A, model 5 was chosen for the simulation experiment as per the conformational stabilization energy value, and the rest of the models were deleted.

Using the leap module of the AMBER 14 software package [468], the input files (topology and coordinate files) of $A\beta_{1-42}$ peptide that are required for molecular dynamics simulation were generated. The $A\beta_{1-42}$ peptide molecule was placed at the center of the simulation box using Packmol [548]. The peptide molecule was then overlaid by equilibrated triple point charge (TIP3P) [480] water molecules with a buffer distance of at least 15 Å between the solute system and the periodic box wall in order to solvate the molecule. Additional positively charged Na^+ counter-ions were added into the system to neutralize the negative charge on the peptide molecule. The $A\beta_{1-42}$ peptide monomer system was then prepared in different ionic strengths of NaCl solution (0.15 M and 0.30 M) by adding 0.15 M and 0.30 M concentrations of Cl^- using the Solvate option of the Amber software package's Leap program. In **Table 4.1**, the numbers of Na^+, Cl^-, and water molecules needed to prepare the corresponding system with desired ionic strength (0 M, 0.15 M and 0.30 M) have been summarized.

4.3.2. Molecular Dynamics Simulation protocol:

The AMBERff99SB force field is used for running the MD simulation [474, 478]. The MD study was done using a standard method that includes heating dynamics, density dynamics, equilibration dynamics, and production dynamics. We used energy-minimized systems as our starting structure for subsequent MD steps. In conditions of constant volume (NVT), the systems were heated slowly from 0 to 300 K. The protein systems were placed in NPT conditions (300 K and 1 atm pressure) for 5 ns to ensure their uniformity. The density procedure was then completed. The protein systems were equilibrated for 5 ns under NPT conditions (300 K and 1 atm pressure). Next, a 40 ns MD production run was performed for the equilibrated structures of three systems, utilizing the Particle Mesh Ewald (PME) algorithm [479] and the 2 fs time step. During the simulation, the non-bonding interactions (short-range electrostatic and van der Waals interactions) were treated with a cut-off of 8 Å and the long-range electrostatic interactions were treated with the PME method. All of the system's bonds were constrained using the SHAKE algorithm [476]. Pressure and temperature (0.5 ps of heat

bath and 0.2 ps of pressure relaxation) were held constant by the Berendsen weak coupling algorithm [477] throughout the simulation protocol. For the three systems, the trajectory snapshots were recorded every 10 ps for further analysis. **Figure 4.1.** shows the Temperature, Pressure and Energy plots $A\beta_{1-42}$ peptide as a function of simulation time for the 0 M NaCl system.

Table 4.1. *Summary of the number of sodium and chloride ions added in the preparation of the three different ionic concentrations of NaCl for the molecular dynamics simulation of $A\beta_{1-42}$ peptide monomer.*

Ionic strength (Concentration in M)	Number of ions of Na^+ added	Number of ions of Cl^- added	No. of water residues present	TIP3P SolvateBOX size (Å)
0 (Control)	3	0	8403	15
0.15	24	24	8403	15
0.30	47	47	8403	15

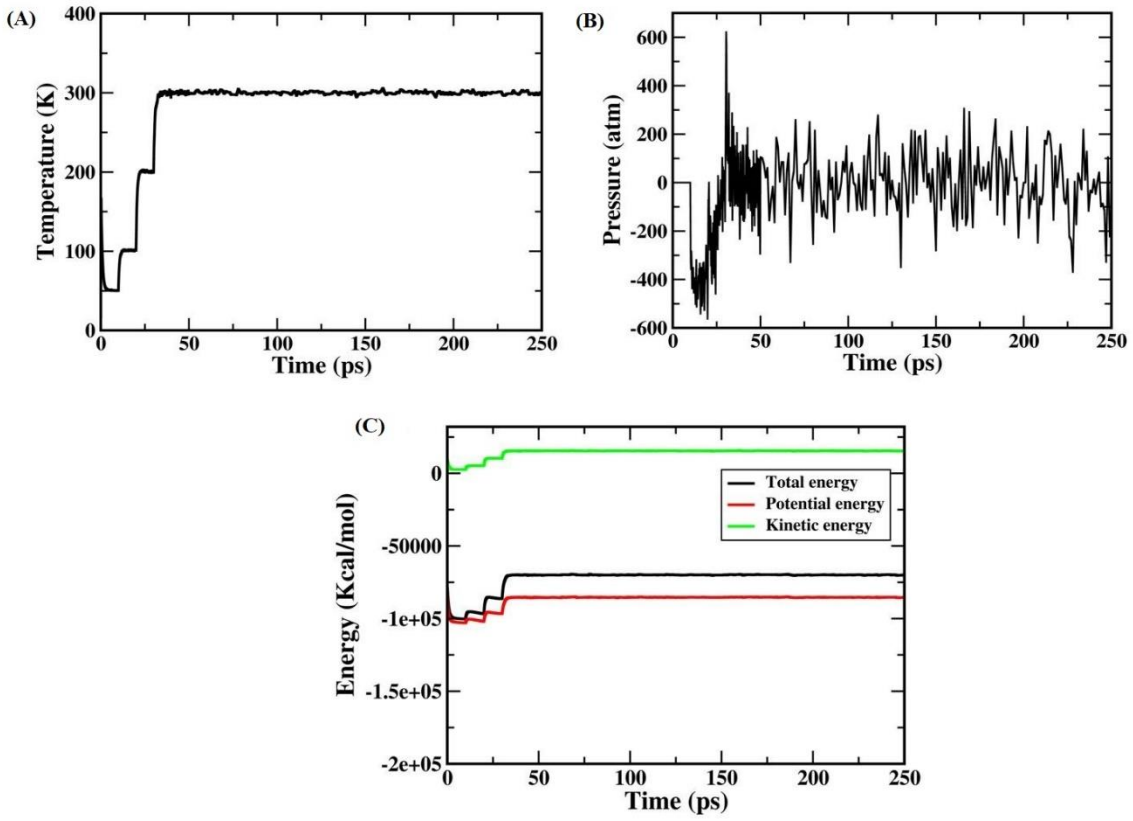

Figure 4.1. *(A) Temperature, (B) Pressure and (C) Energy plots of $A\beta_{1-42}$ peptide as a function of simulation time for the 0 M NaCl system.*

4.3.3. Analysis of the MD Trajectories:

To investigate the effect of ionic strength on the conformational dynamics of the $A\beta_{1-42}$ peptide, $A\beta_{1-42}$ peptide was placed in NaCl solutions of three different ionic strengths (0 M, 0.15 M, and 0.30 M) and molecular dynamics simulations were performed. Using the CPPTRAJ algorithm [549] of the AMBER 14 software package, RMSD, RMSF, B-factor, SASA, and R_g plots from the corresponding MD trajectories, as well as snapshots at different time intervals with reference to their initial built structures were analyzed.

4.4. Results and discussion:

4.4.1. Interpretations of MD Trajectories for $A\beta_{1-42}$ Peptide in the three Explicit Systems:

Root Mean Square Deviation (RMSD) analysis: For each of the three different systems, the RMSD values of all of the C_α-atoms were compared to their initial structures in order to determine whether or not they had reached a stable state. **Figure 4.2(A)** presents a visual representation of the RMSD plots obtained for each of the three systems. In comparison to the $A\beta_{1-42}$ peptide found in the other two explicit systems, the $A\beta_{1-42}$ peptide found in the solution containing 0 M NaCl was observed to be well settled throughout the simulation. While the $A\beta_{1-42}$ peptide in 0.15 M and 0.30 M NaCl solution showed initial stability at an RMSD of 4 Å, after which it deviated and maintained a gradual slope thereafter. Thus, it can be inferred that $A\beta_{1-42}$ peptide undergoes significant conformational changes in the three cases of different ionic strengths and attain stability at approximately 10,000-30,000 ps, at an RMSD of 8-10 Å, and maintain a gradual slope thereafter.

Radius of Gyration (R_g) analysis: R_g is usually calculated to estimate the overall dispersion of atoms in a particular biomolecule from their common center of gravity or axis. The R_g analyses of the $A\beta_{1-42}$ peptide in the three systems of different ionic strengths are shown in **Figure 4.2(B)**. Here, we observed that the R_g values for the $A\beta_{1-42}$ peptide in 0 M NaCl solution take higher values (~20 Å) while the R_g values for $A\beta_{1-42}$ peptide dissolved in 0.15 M and 0.30 M NaCl solution exhibit lower values (~13-15 Å) and remain stable. Thus, it can be inferred that the structure of $A\beta_{1-42}$ peptide in 0 M

NaCl solution was relatively less compact than in 0.15 M and 0.30 M NaCl solutions. The changes we observed in the R_g values reflect the structural changes that have taken place in $A\beta_{1-42}$ peptide monomer during the course of the simulation time.

Root Mean Square Fluctuation (RMSF) analysis: To obtain information on local structural flexibility, thermal stability, and heterogeneity of macromolecules, and Root Mean Square Fluctuations (RMSF) are often studied. In our simulation experiment, we examined the RMSF values for the C- atom of the $A\beta_{1-42}$ peptide in three different ionic configurations (0 M, 0.15 M, and 0.30 M) to determine the peptide's local deformability. From the RMSF analysis shown in Figure 4.2(C), it can be inferred that the ionic strength of the solution has a considerable effect on the structural flexibility of $A\beta_{1-42}$ peptide monomer.

Solvent Accessible Surface Area (SASA) analysis: The SASA analyses of the $A\beta_{1-42}$ peptide in the three systems of different ionic strengths are shown in Figure 4.2(D). To map out the surface area accessible by the water solvent in the three systems under study, we had used a probe with a radius of 1.4 Å. The SASA of the $A\beta_{1-42}$ peptide monomer dissolved in 0 M NaCl solution was initially mapped in the range of 4,000-4,500 $Å^2$, which later shifted to 4250-4700 $Å^2$, thus showing the relatively larger accessible surface area than $A\beta_{1-42}$ peptide dissolved in 0.15 M and in 0.30 M NaCl solution. This increase can be attributed to the increase in the hydrophobic contacts within the peptide. Therefore, it can be seen that the accessible surface area of the $A\beta_{1-42}$ peptide changes rapidly during the course of the simulation period.

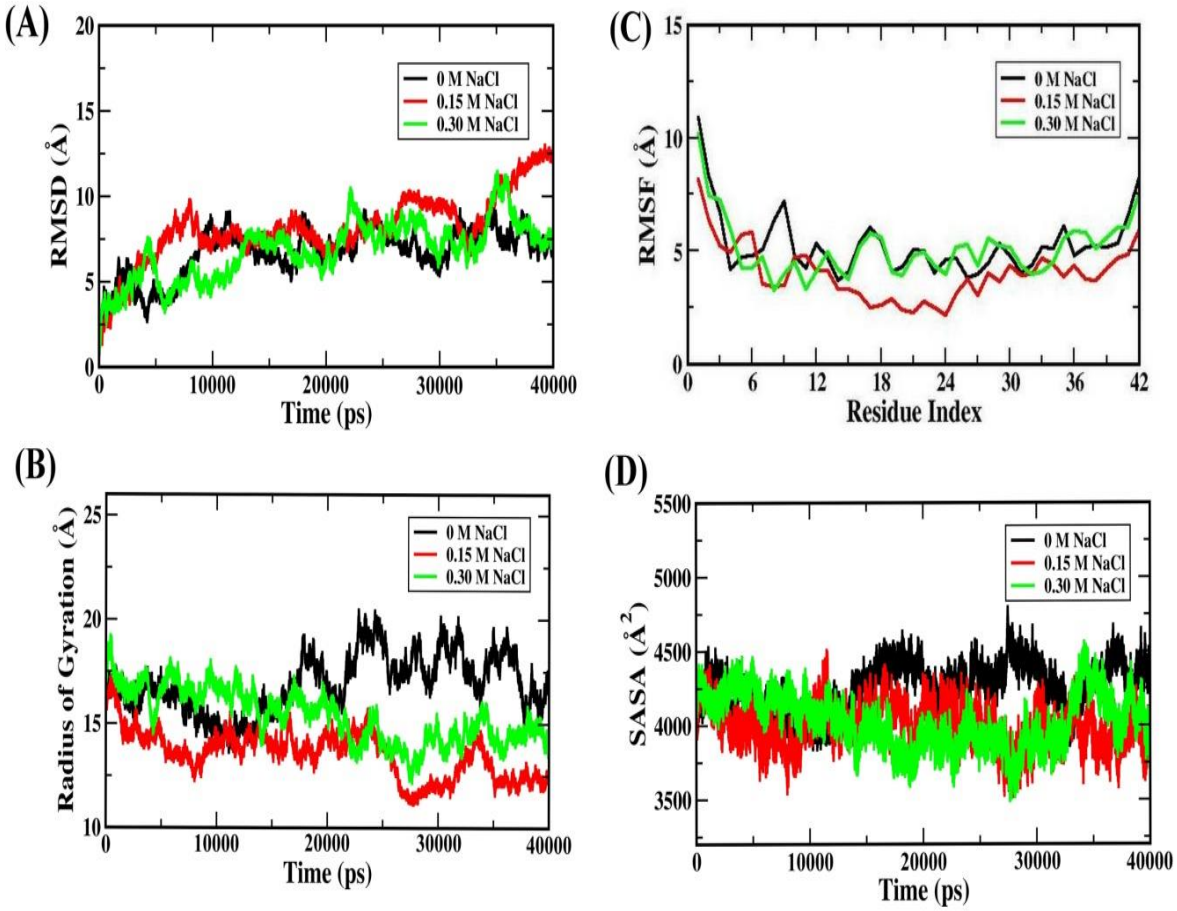

Figure 4.2. *Comparative MD analyses of (A) Root mean square deviation, (B) Radius of gyration, (C) Root mean square fluctuation, and (D) Solvent accessible surface area of* $A\beta_{1\text{-}42}$ *peptide in the three different ionic concentrations of NaCl (0 M, 0.15 M and 0.30 M).*

4.4.2. Analysis of Secondary Structure:

The secondary structure analysis for $A\beta_{1\text{-}42}$ peptide in the three systems of different ionic strengths was carried out using the Kabsch and Sander algorithm incorporated in their DSSP (Dictionary of Secondary Structure for Protein) program [532]. From the graph (**Figure 4.3**), it has been observed that at higher ionic strength (0.15 M and 0.30 M) of the solution, α-helical secondary structure present in the $A\beta_{1\text{-}42}$ peptide monomer is retained well during the course of the simulation. The plot (**Figure 4.3**) depicts the probable secondary structure that corresponding residues of $A\beta_{1\text{-}42}$ peptide can have at different ionic strengths of solution. It has been found that α-helical content is predominant in $A\beta_{1\text{-}42}$ peptide monomer structure at a higher ionic strength of

the solution. It is also found that anti-parallel β-sheets in $A\beta_{1-42}$ peptide decrease with the increase in ionic strength of the solution.

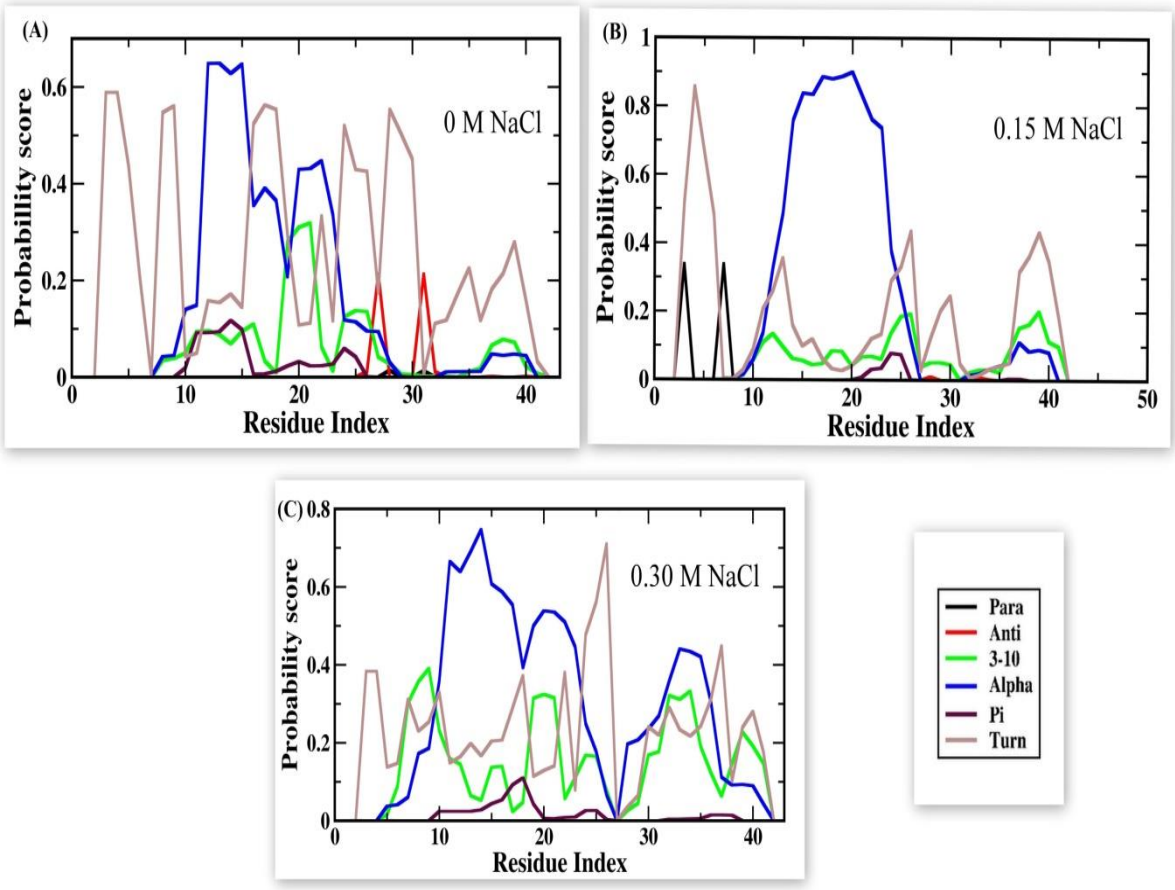

Figure 4.3. *Probability score of secondary structure for $A\beta_{1-42}$ peptide in different ionic concentrations;(A) 0 M NaCl, (B) 0.15 M NaCl, and (C) 0.30 M NaCl solution.*

4.4.3. Analysis of Conformational Snapshots:

To further strengthen our study, we extracted the conformational snapshots of the $A\beta_{1-42}$ peptide from the MD trajectories at 0, 10, 20, 30, and 40 ns. **Figure 4.4** shows the conformational snapshots of the $A\beta_{1-42}$ peptide dissolved in 0 M, 0.15 M, and 0.30 M NaCl solutions. In **Figure 4.4**, the amount of helices portion was observed to be relatively higher in $A\beta_{1-42}$ peptide monomer structure placed in higher ionic strength (0.15 M and 0.30 M) of the NaCl solution. And the structure of $A\beta_{1-42}$ peptide was observed to undergo folding when it is placed in the solution of moderate ionic strength (0.15 M). The structure of $A\beta_{1-42}$ peptide monomer was found to undergo unfolding to a greater extent in lower ionic strength than in the higher ionic strength of NaCl solution.

This could explain why the $A\beta_{1-42}$ peptide monomer structure contains more helical segments when placed in NaCl solutions with higher ionic strengths (0.15 M and 0.30 M). The average structure of $A\beta_{1-42}$ peptide at different ionic strengths are depicted in **Figure 4.5**. Therefore, it is observed that the ionic strength of the solution plays an important role in affecting the aggregation propensity of the $A\beta_{1-42}$ peptide.

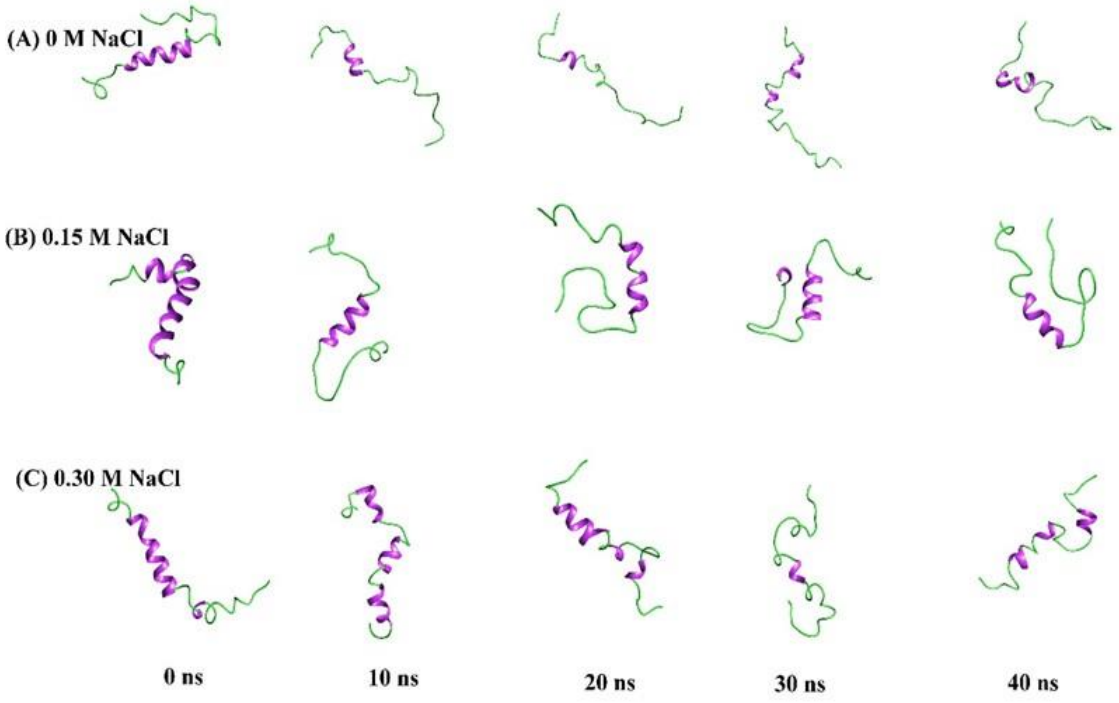

Figure 4.4. *Conformational snapshots of $A\beta_{1-42}$ peptide monomer in three different ionic concentrations of NaCl (A)0 M, (B)0.15 M and (C)0.30 M at different time intervals of simulation time.*

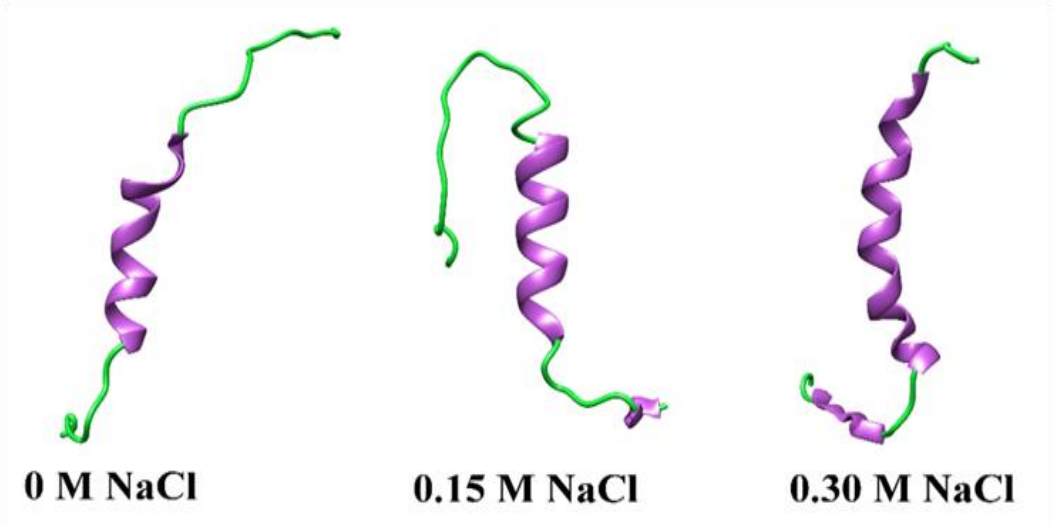

Figure 4.5. *Average structures of $A\beta_{1-42}$ peptide at 0 M, 0.15M and 0.30 M NaCl solution.*

4.4.4. Analysis of Hydrogen bonds:

Additionally, the intra-molecular hydrogen bonds of $A\beta_{1-42}$ peptide (defined by the distance between donor and acceptor being less than or equal to 3.5 Å and the angle between acceptor, donor, and hydrogen being less than 30 degrees) formed during the simulation period **(Figure 4.6**) have also been analyzed. These hydrogen bonds play a crucial role in conferring the stability of the $A\beta_{1-42}$ peptide. The average number of hydrogen bonds present in $A\beta_{1-42}$ peptide at different ionic strengths from the entire simulation period has been calculated. The average number of hydrogen bonds present in $A\beta_{1-42}$ peptide was found to be 10, 12, and 15 in 0 M, 0.15 M, and 0.30 M NaCl solution, respectively. With the increase in the ionic strength of the solution, the number of hydrogen bonds in $A\beta_{1-42}$ peptide was found to be increasing. The average distance and angle of the hydrogen bonds, as well as the names of the residues that helped make the hydrogen bonds, were calculated.

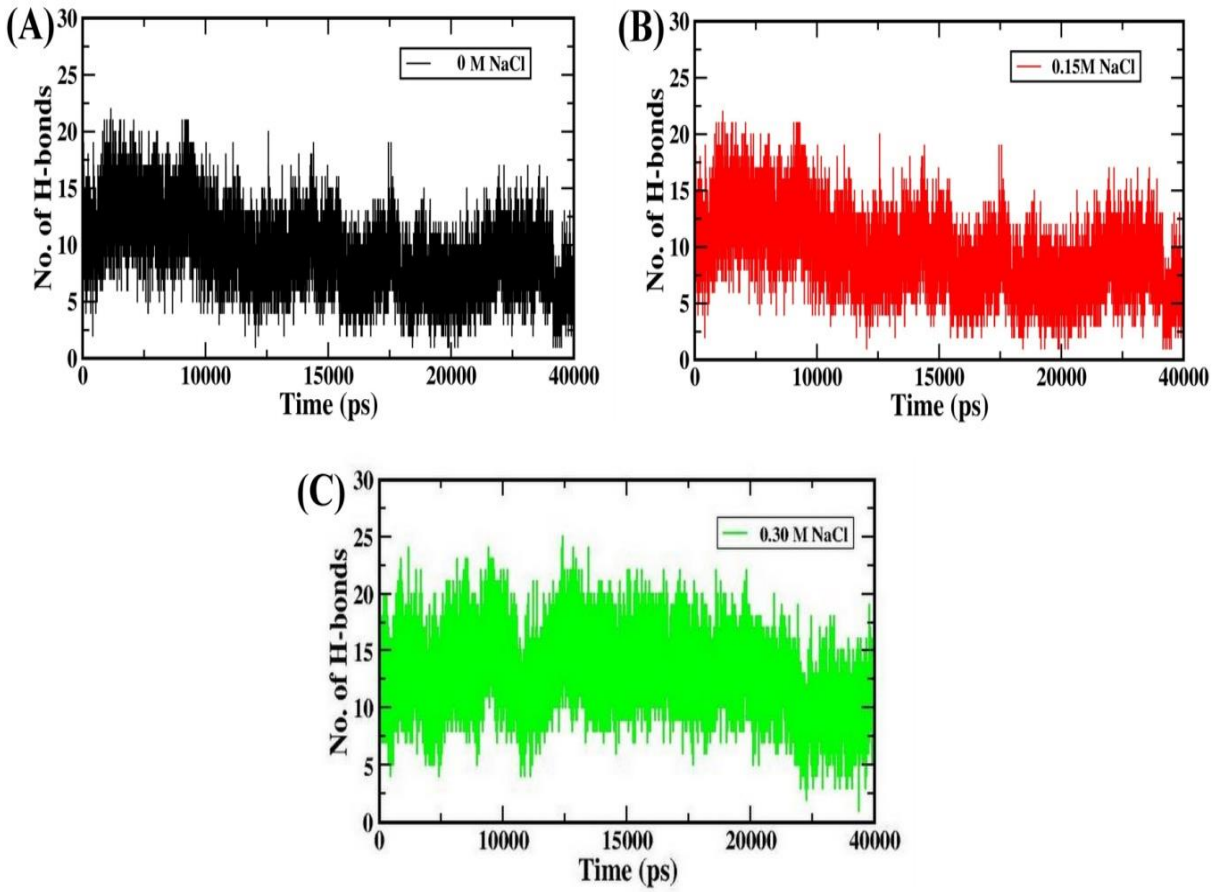

Figure 4.6. *Hydrogen Bond analysis for $A\beta_{1-42}$ peptide monomer in three different ionic concentrations of NaCl (A) 0 M, (B) 0.15 M and (C) 0.30 M as a function of simulation time in picoseconds.*

The occupancies of the hydrogen bond formation amongst the $A\beta_{1-42}$ peptide in the three explicit systems, along with their respective bond distances and bond angles, are provided in **Tables 4.2, 4.3, and 4.4**. We found that many intra-molecular hydrogen bonds have been destabilized with the increase in the ionic strength of the solution. This is in agreement with the experimental data of amyloid oligomerization [550]. Therefore, we observed that the change in ionic strength of solution affects the internal hydrogen bonds in $A\beta_{1-42}$ peptide monomer. *Kriz et al*. have also noticed a similar trend in the internal hydrogen bonds with a change in ionic strength on the conformational behavior of human and rat amyloids [551].

Table 4.2*. Intramolecular Hydrogen bond occupancy of $A\beta_{1-42}$ peptide at 0 M NaCl solution*

Acceptor	Donor	Fraction	Average Distance (Å)	Average Angle (°)
GLU_11@O	GLN_15@N	0.36	2.877	159.9742
HIE_14@O	VAL_18@N	0.36	2.8909	160.6616
GLU_3@OE1	GLU_3@N	0.255	2.8535	151.4693
HIE_14@O	LEU_17@N	0.25	2.8956	153.7391
PHE_19@O	ASP_23@N	0.25	2.8901	159.0257
GLU_3@OE2	GLU_3@N	0.235	2.8616	151.9724
GLN_15@O	PHE_19@N	0.225	2.8662	152.3569
GLU_11@O	HIE_14@N	0.205	2.8826	150.3821
VAL_12@O	LYS_16@N	0.2	2.9005	158.4942
GLU_3@OE2	ASP_1@N	0.175	2.8093	152.1761
GLU_3@OE1	ASP_1@N	0.17	2.8369	155.2793
PHE_20@O	GLY_25@N	0.17	2.8702	162.6363

GLU_3@OE1	ASP_1@N	0.165	2.8083	154.8665
PHE_19@O	GLU_22@N	0.165	2.8695	155.4863
GLU_3@OE1	ASP_1@N	0.155	2.8115	151.2088
ASP_7@OD1	GLY_9@N	0.15	2.891	157.0087
ASP_7@OD2	GLY_9@N	0.15	2.876	153.7261
GLU_3@OE2	ASP_1@N	0.145	2.7924	151.6256
TYR_10@O	GLN_15@N	0.145	2.839	154.6477
ALA_2@O	ARG_5@N	0.135	2.8982	149.7502
TYR_10@O	HIE_14@N	0.135	2.8826	156.5465
ASP_23@OD2	SER_26@OG	0.135	2.6814	163.9939
ASN_27@O	ILE_31@N	0.135	2.8832	161.9834
LEU_34@O	VAL_36@N	0.135	2.8142	145.7483
PHE_20@O	VAL_24@N	0.13	2.8946	150.7008
ASP_23@O	SER_26@N	0.125	2.9083	152.2242
ASN_27@O	ALA_30@N	0.125	2.9044	154.3046
GLU_3@OE2	ASP_1@N	0.12	2.8244	147.9597
ASP_23@OD1	SER_26@OG	0.115	2.7066	167.0381
ASP_7@OD2	TYR_10@OH	0.105	2.6895	164.77

Table 4.3. *Intramolecular Hydrogen bond occupancy of $A\beta_{1-42}$ peptide at 0.15 M NaCl solution.*

Acceptor	Donor	Fraction	Average Distance (Å)	Average Angle (°)
LEU_17@O	ALA_21@N	0.4677	2.8778	158.2632
PHE_20@O	VAL_24@N	0.3462	2.8951	159.1915
HIE_14@O	VAL_18@N	0.34	2.8867	162.4375
ALA_2@O	HIE_6@N	0.3292	2.8728	157.6635
GLU_22@O	SER_26@OG	0.3015	2.7334	163.5729
VAL_36@O	VAL_39@N	0.3	2.8946	157.2635
GLN_15@O	PHE_19@N	0.2723	2.8817	156
GLU_3@OE2	GLU_3@N	0.2662	2.8427	147.9226
PHE_19@O	ASP_23@N	0.2631	2.8947	155.0705
LYS_16@O	PHE_20@N	0.2585	2.8861	159.0007
GLU_11@O	GLN_15@N	0.2354	2.8805	161.974
ASP_7@O	PHE_4@N	0.2292	2.828	150.9753
GLU_3@OE1	GLU_3@N	0.2262	2.8513	149.4185
ALA_2@O	ASP_7@N	0.2123	2.8932	160.4964
ASP_7@OD2	GLY_9@N	0.1908	2.8697	158.5982
ASP_7@OD1	GLY_9@N	0.1862	2.8793	157.0783
VAL_12@O	LYS_16@N	0.1677	2.8944	157.726
GLU_3@OE1	ASP_1@N	0.1631	2.8014	154.6171

GLU_3@OE1	ASP_1@N	0.1523	2.811	153.2267
GLU_11@O	HIE_14@N	0.1523	2.8748	151.6132
GLU_3@OE1	ASP_1@N	0.1462	2.8134	155.1208
GLU_3@OE2	ASP_1@N	0.1446	2.8165	153.4362
PHE_20@O	GLY_25@N	0.1369	2.872	160.8555
GLU_3@O	ARG_5@N	0.1277	2.8166	146.0662
HIE_13@O	LEU_17@N	0.1262	2.8953	159.5029
ASN_27@OD1	GLY_29@N	0.1246	2.8927	155.4779
VAL_18@O	GLU_22@N	0.12	2.893	157.4916
ALA_2@O	ARG_5@N	0.1169	2.8903	150.4246
ALA_21@O	GLY_25@N	0.1169	2.8731	152.0315
GLU_3@OE2	ASP_1@N	0.1138	2.8245	155.5101

Table 4.4. *Intramolecular Hydrogen bond occupancy of $A\beta_{1-42}$ peptide at 0.30 M NaCl solution*

Acceptor	**Donor**	**Fraction**	**Average Distance (Å)**	**Average Angle (º)**
ASP_7@OD2	ARG_5@NH2	0.4067	2.7946	159.8679
TYR_10@O	HIE_14@N	0.3578	2.8634	159.0275
GLU_11@O	GLN_15@N	0.3489	2.8834	161.3424
HIE_14@O	VAL_18@N	0.3	2.8821	161.1603
ASP_7@OD1	ARG_5@NE	0.2911	2.8341	160.0983

PHE_19@O	ASP_23@N	0.2756	2.8767	156.9723
ASP_7@OD2	ARG_5@NE	0.2578	2.8528	158.7741
LEU_17@O	ALA_21@N	0.2422	2.8747	157.1156
GLU_11@OE1	ARG_5@NH2	0.24	2.806	158.7091
HIE_14@O	PHE_19@N	0.24	2.8812	161.7014
TYR_10@O	HIE_13@N	0.2356	2.8753	151.0386
GLU_3@OE2	GLU_3@N	0.2311	2.864	152.5557
ASP_7@OD1	ARG_5@NH2	0.2311	2.7932	160.5852
ASN_27@OD1	GLY_29@N	0.2178	2.8734	151.4968
GLU_11@OE2	ARG_5@NH2	0.1956	2.7967	158.9743
ASP_23@O	ASN_27@N	0.1844	2.8532	157.4292
GLU_11@OE1	ARG_5@NH1	0.1822	2.8131	155.5255
GLY_33@O	GLY_37@N	0.1822	2.8629	152.5215
HIE_13@O	LEU_17@N	0.18	2.8818	156.4803
LYS_16@O	PHE_20@N	0.1778	2.8859	159.4259
VAL_18@O	GLU_22@N	0.1733	2.8755	159.2425
ILE_31@O	LEU_34@N	0.1689	2.8944	151.7653
ILE_32@O	MET_35@N	0.1689	2.8855	151.7176
GLU_3@OE1	GLU_3@N	0.1667	2.859	155.2885

PHE_20@O	VAL_24@N	0.1644	2.8717	159.3806
ILE_31@O	MET_35@N	0.1489	2.8965	157.8083
GLU_11@OE2	ARG_5@NH1	0.1422	2.8254	155.5141
GLN_15@O	PHE_19@N	0.1378	2.8751	152.2062
GLU_22@O	SER_26@OG	0.1378	2.7224	164.1507
GLU_3@OE1	ASP_1@N	0.1356	2.8082	153.9177

4.4.5. Analysis of Diffusion Coefficient:

To calculate the self-diffusion coefficient of $A\beta_{1-42}$ peptide monomer in different ionic strengths of the solution, we have used the Einstein relation, as shown in equation 4.1.

$$D = 1\ 6 \lim t \rightarrow \infty\ d/dt <MSD> \quad \textbf{(4.1)}$$

Where, <MSD> represents averaged mean square displacement. However, because of the linear relationship between MSD> and time t, graphical methods can be used to calculate D using the relation MSD=2nDt, where n represents the dimension. The slope calculated from the graph (**Figure 4.7**) plotted between <MSD> and time for the $A\beta_{1-42}$ peptide monomer in different ionic strength is summarized in **Table 4.5**. The Diffusion coefficient value for $A\beta_{1-42}$ peptide in 0 M NaCl solution was found to be lower as compared to the value observed in 0.15 M NaCl solution. However, the diffusion co-efficient value for $A\beta_{1-42}$ peptide in 0.30 M NaCl solution tends to decrease, which is probably due to structural changes developed in the molecule. Miao Yu et al. [552] did an experiment that showed a similar diffusion pattern. At similar concentration gradients, they found that the measured lysozyme diffusion coefficient decreased by a large amount as the ionic strength increased. The diffusivity values of $A\beta_{1-42}$ peptide noticed in this study at different ionic strengths indicate a probable effect on its aggregation propensity.

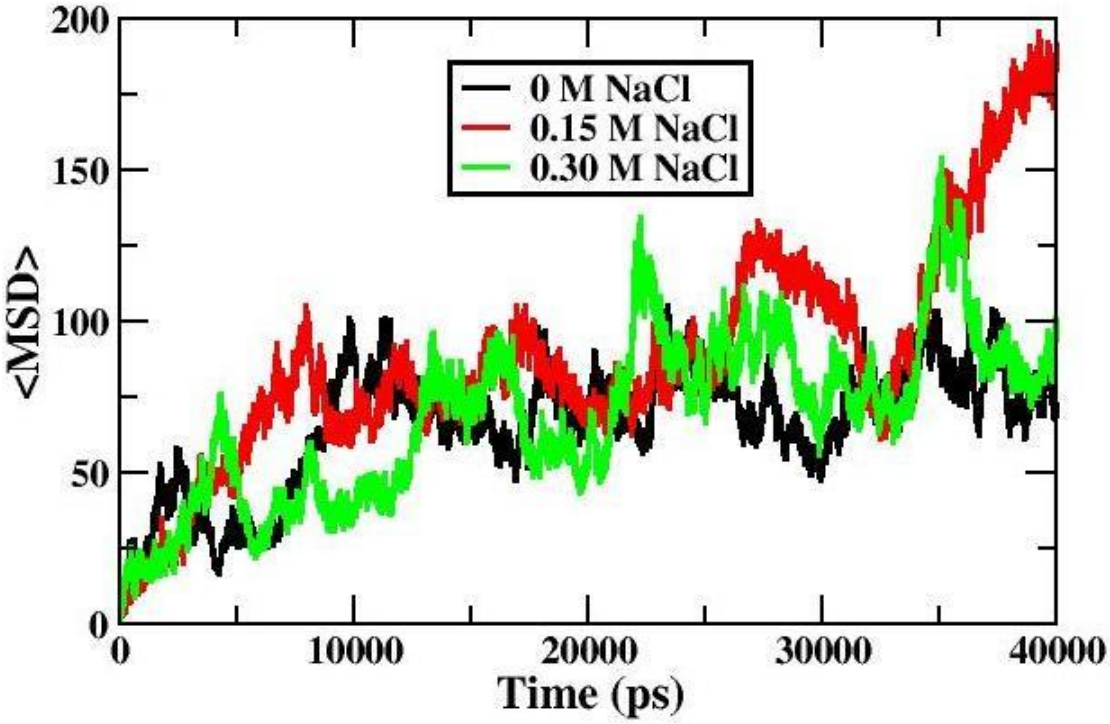

Figure 4.7. *Mean Square Deviation vs Time (ps) plot of $A\beta_{1-42}$ peptide at 0 M, 0.15 M and 0.30 M NaCl solution.*

Table 4.5. *Comparison of diffusion coefficient values for $A\beta_{1-42}$ peptide at different ionic concentrations of NaCl (0 M, 0.15 M and 0.30 M) solution.*

Concentration (M)	**Slope**	**Diffusion Coefficient(D) (Unit: m^2/s)**
0	0.0022	0.0037
0.15	0.0054	0.0090
0.30	0.0037	0.0062

4.5. Conclusion:

Our computational investigation into the effect of ionic strength on the aggregation propensity of $A\beta_{1-42}$ peptide has yielded numerous insights into the role of ionic strength in determining the stability of $A\beta_{1-42}$ peptide. The MD trajectory analysis reveals that the structural tendency of $A\beta_{1-42}$ peptide monomer to undergo aggregation decreases as the ionic strength of the solution increases. RMSD and SASA analysis revealed that the $A\beta_{1-42}$ peptide monomer undergoes a rapid change in conformation as the ionic strength of the solution rises. This observation is consistent with the R_g

analysis, which confirms that the $A\beta_{1-42}$ peptide monomer is more compact when the solution's ionic strength is moderate. The $A\beta_{1-42}$ peptide monomer also retains its helical secondary structure when the ionic strength of the solution is moderate or greater. This is consistent with the beta-barrel models of amyloid oligomers published by Shafrir et al. [553] and the amyloid beta fibril stability published by Zidar et al. [554]. In addition, the diffusion coefficient of $A\beta_{1-42}$ peptide monomer is found to be greater in solutions with moderate ionic strength. In conclusion, the findings of this computational study highlight the marked effect of the ionic strength of the solution on the aggregation propensity of $A\beta_{1-42}$ peptide monomer and thus provide potential avenues for the prevention of AD through the inhibition of $A\beta_{1-42}$ peptide aggregation.